Al-Azhar University Civil Engineering Research Magazine (CERM)
Vol. (40) No. (4) October, 2018

Nonlinear FE Analysis of Steel-Concrete Composite Beam-to-Column Joints Subjected to Monotonic Loading

Eng. A. M. Khalil, Assoc. Prof. Dr. E. S. Salem, Prof. Dr. S. A. Hassanein

Al-Azhar University, Faculty of Engineering, Civil Engineering Department

ملخص البحث

فى هذا البحث, يتم تقديم دراسه تحليليه لسلوك الوصلات بين الكمر والعمود فى المنشأت المركبه من حديد وخرسانه.والنتائج التفصيليه للاختبارات المعمليه لنموذج معرض لقوى جانبيه والتى اجريت فى جامعه بيزا-ايطاليا[1]. كما يتم مناقشة الدراسات العدديه التى اجريت من اجل فهم سلوك النموذج وعلى وجه الخصوص التركيز على الدور الذى تقوم به البلاطه الخرسانيه فى زياده قدره الوصلات بين الكمر والعمود فى المنشأت المركبه من حديد وخرسانه على نقل قوى الضغط الواقعه على تلك النوع من الوصلات نتيجه الاحمال الجانبيه. ويتم عرض نماذج ثلاثيه الابعاد لوصله داخليه معرضه لحمل جانبى.ويؤخذ فى الحسبان خصائص المواد الغيرخطيه للاعمده والبلاطه الخرسانيه وحديد التسليح والتى تمثل النقاط الحرجه للاداء المشترك. ويتم تقديم مقارنه بين نتائج الاختبار العملى والتحليل العددى والتى اظهرت اتفاقا معقولا بين النتائج العملية والتحليل العددى.

Abstract

In this research, the behavior steel composite beam-to-column connection is numerically studied. Experimental results from full-scale sub-assemblages monotonic test, performed at the Laboratory for Materials and Structures Testing, University of Pisa, Italy [1], were used to verify the finite element model. This investigation is focused on the role of the concrete slab in enhancing the behavior of composite beam-to-column connection. Based on the approach proposed by the Eurocode 8, the bearing capacity of the concrete slab in compression is globally schematized using strut & tie mechanism. To better understand this mechanism, 3D FE models of exterior and interior joints were developed, using ABAQUS software, and validated against the experimental investigations conducted at the University of Pisa, Italy [1]. Comparison between FE results and test data shows a reasonable agreement. Finally, from this study, it can be concluded that the connection between steel beam and column, and concrete compressive strength are the main parameters affecting the behaviour of the joint.

Keywords: Steel–concrete composite structure, composite joint; numerical modeling, strut and tie.

1. Introduction

Steel–concrete composite structures can provide high level of performance in terms of ductility and energy dissipation, while at the same time reducing construction costs. Composite structures have been increasingly applied in buildings. The effective application of steel and concrete leads to increasing the strength and stiffness compared to traditional solutions such as bare steel or reinforced concrete structural elements. Due to the advances in composite construction, the scope of application of composite actions in steel frameworks has been widened to include composite joints. Design rules for composite joints were developed as a result of limited guidance in this field [2].

Composite connections are greatly influenced by the behaviour of end-plates and bolts [3].

Lee and Lu [4] studied composite beam-to-column joint substructures by means of the ADINA software [5]. Two-step approach was used. Firstly, a three-dimensional (3D) elastic analysis of a composite joint beam was carried out to determine the effective slab width. Secondly, a two-dimensional (2D) inelastic analysis of the joint substructure was done to study the effect of composite action in both the slab and column web panel zone. This approach implies that the effective width of the slab does not greatly differ between elastic and inelastic regimes.

Hajjar et al. [6] proposed a 3D modeling of interior beam-to-column composite connections with angles by means of the ABAQUS [7]. Doneaux [8] modeled exterior beam-to-column composite joints with and without transverse beam by thin shell elements using CASTEM 2000[9]. The slab was modeled with multi-layered thin shells; the concrete model combined a Rankine fixed crack model for tension and an elastoplastic law with Drucker–Prager criteria for compression; and shear connectors were modeled by means of beam elements. Bursi and Ferrario [10] investigated several analysis and modelling issues in composite joints, composite beams and moment-resisting (MR) frames. They adopted one-dimensional (1D) models relying on layered beam-column elements [11]. All models took into account the nonlinear behaviour of concrete, steel, stud shear connectors and of steel–concrete force-slip relationships, showing that the performance of composite beams with full and partial shear connection and full and partial-strength joints was satisfactory both in terms of strength and of ductility.

2. Description of Beam-To-Column Joint

In this section, details of the experimental specimen, tested by L. Sim˜oes et al. [2], used to verify the finite element model, are presented. Full-scale sub-assemblage specimen for an interior joint was tested. Figure 1 shows the test setup used for the interior joint.

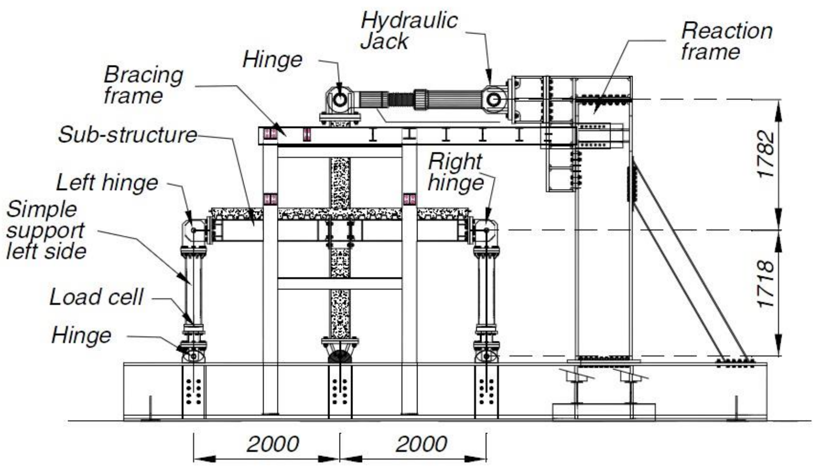

Figure 1 Sub assemblage experimental setup (interior joint) [23]

As shown in Figures. 2(a)-(d), the beams are made of IPE300 sections that acting compositely with the 150 mm thick concrete slab. The slab is poured on a 55 mm deep trapezoidal composite steel deck. Shear studs, arranged in pairs, are used at every rib to ensure composite action with the beams. The slab was reinforced by a steel mesh and longitudinal rebars were placed on each side of the column to resist negative (hogging) bending moments.

At the column face, only the upper 95mm portion of the slab was bearing against the steel column (Figure. 2(a)). Transverse rebars were used at the column faces to resist the tension forces that develop perpendicular to the beam axis.

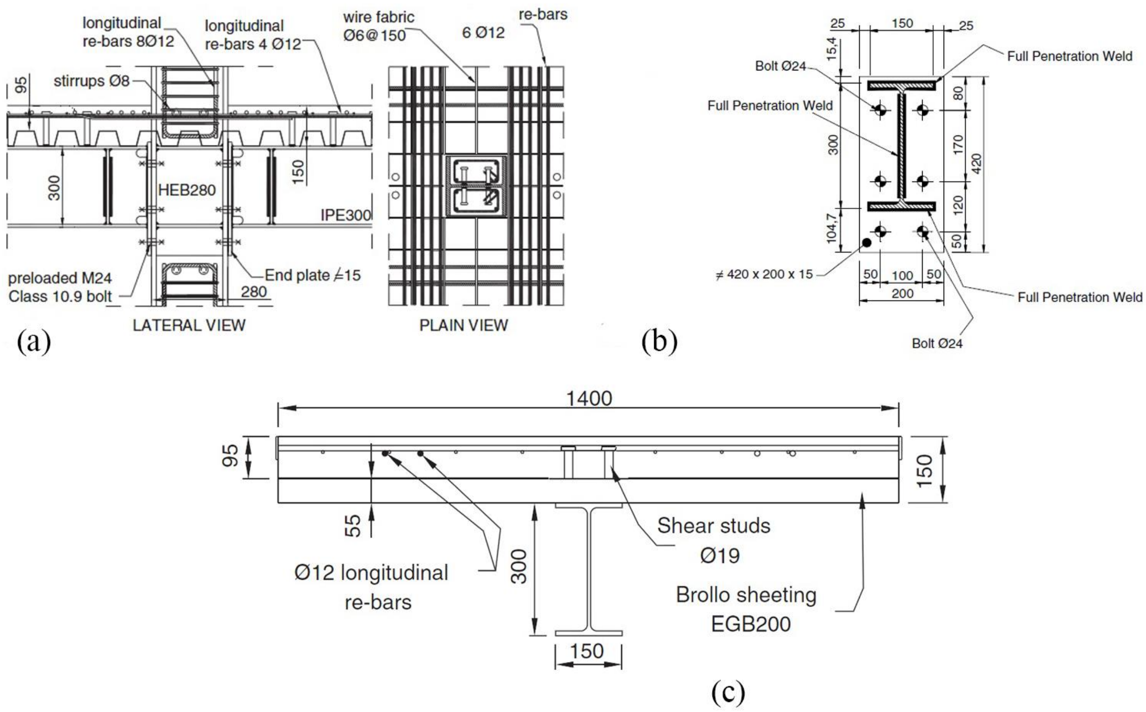

Figure 2 Beam–column specimens: (a) interior joint; (b) geometrical details of end plate; and (c) cross-section of the composite beam[23].

Precast partially encased composite column was used for the joint, as shown in Figure 2(a).

The beam-to-column joint has been designed to provide adequate structural performance under monotonic Loading [12]. The design material properties are S235 for structural steel, C25/30 for concrete, and B450-C for reinforcing bars. More Details information on the joint material can be found in Reference [12].

3. Finite Element Numerical Modeling

The structural behaviour of full-scale composite beam-to-column joints subjected to monotonic loading has been investigated using a three-dimensional FE model. In this study, ABAQUS/CAE software [7] was employed to develop the FE analysis. Material and geometrical non-linearities, as well as the non-linearity associated with contacts/interfaces, were incorporated in the model. Because of the symmetry of the specimens and loading, only one half of the specimen considered.

3.1 Material Constitutive Relationship

The stress-strain characteristics of the materials used in the composite joints are modeled

using empirical constitutive laws, and are described in the following sections.

3.1.1. Concrete Model

Concrete damage plasticity (CDP) is one of the possible constitutive models to predict the constitutive behavior of concrete. It describes the constitutive behavior of concrete by introducing scalar damage variable. The tensile and compressive response of concrete can be characterized by CDP as shown in Figure 3.

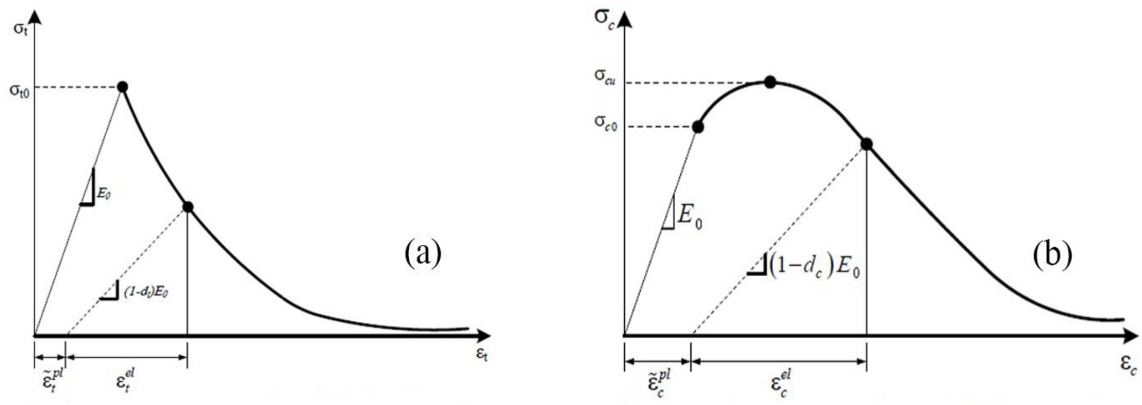

Figure.3 Behavior of concrete under axial tension (a) and (b) compression [7]

As shown in Figure 3, the unloaded response of concrete specimen seems to be weakened because the elastic stiffness of the material appears to be damaged or degraded. The degradation of the elastic stiffness of the stress-strain curve is characterized by two damage variables, d_t and d_c , which can take values from zero to one. Zero represents the undamaged material where one represents a total loss of strength [7]. E_0 is the initial (undamaged) elastic stiffness of the material and $\tilde{\varepsilon}_c^{pl}, \tilde{\varepsilon}_t^{pl}, \tilde{\varepsilon}_c^{in}, \tilde{\varepsilon}_t^{in}$ are compressive plastic strain, tensile plastic strain, compressive inelastic strain, and tensile inelastic strain respectively. The stress-strain relations under uniaxial tension and compression are taken into account in Equations (1) and (2).

$$\sigma_t = (1 - d_t).\mathrm{E}_0.(\varepsilon_t - \tilde{\varepsilon}_t^{pl}) \quad (1)$$

$$\sigma_c = (1 - d_c).\mathrm{E}_0.(\varepsilon_c - \tilde{\varepsilon}_c^{pl}) \quad (2)$$

Interface behaviour between rebar and concrete is modeled by implementing tension stiffening in the concrete modeling to simulate load transfer across the cracks through the rebar. Tension stiffening also allows to model strain softening behaviour for cracked concrete.

In ABUQUS [7], fracture energy approach can be used instead of post-failure stress-strain relation. In this approach, the amount of energy (*GF*) which is required to open a unit area of a crack is assumed as a material property. Thus, concrete's brittle behavior is defined by stress-displacement response rather than a stress-strain response. Specifying the post-failure stress versus corresponding cracking displacement is enough to describe this approach as shown in Figure 4 [7].

As an alternative, GF can be implemented directly as a material property. However, in this case, a linear loss of strength after cracking is assumed (Figure 4(b)). From CDP perspective, ABAQUS [7] automatically calculates both plastic displacement values using Equations (3) and (4).

$$u_t^{pl} = u_t^{ck} - \frac{d_t}{(1-d_t)} \frac{\sigma_t I_0}{\mathrm{E}_0} \tag{3}$$

$$\tilde{\varepsilon}_c^{pl} = \tilde{\varepsilon}_c^{in} - - \frac{d_c}{(1-d_c)} \frac{\sigma_c}{\mathrm{E}_0} \tag{4}$$

From these equations "effective" tensile and compressive cohesion stresses ($\bar{\sigma}_{t,c}$) can be defined as:

$$\bar{\sigma}_t = \frac{\sigma_t}{(1-d_t)} = \mathrm{E}_0(u_t - u_t^{pl}) \tag{5}$$

$$\bar{\sigma}_c = \frac{\sigma_c}{(1-d_c)} = \mathrm{E}_0(\varepsilon_c - \tilde{\varepsilon}_c^{pl}) \tag{6}$$

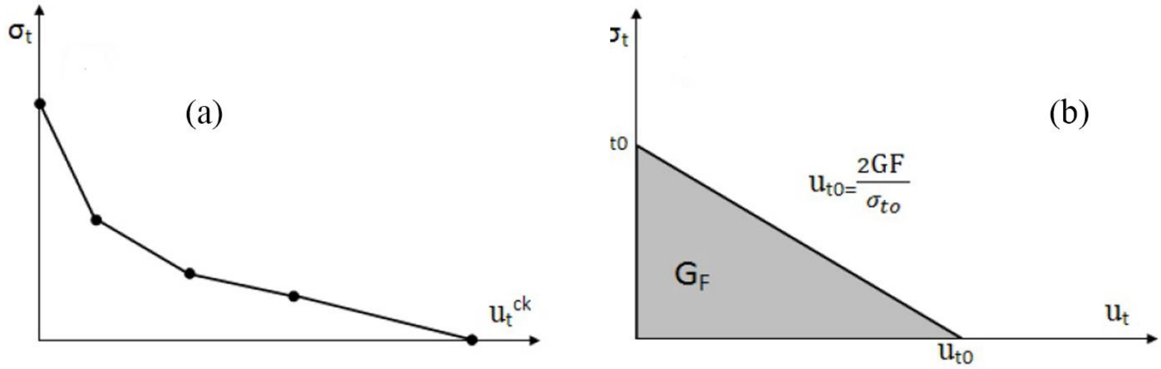

Figure 4 Post-failure stress-strain relation with fracture energy approach [7]

Property value for the assumed model of concrete was selected from the full-scale test results conducted in the laboratory of the University of Pisa, Italy [2]. According to the characteristics of concrete after 28 days, the compressive strengths of concrete, f_{cm} , is 37.57 MPa .

3.1.2. Structural Steel, High Strength Bolts and Reinforcing Bars

Material non-linearity was included in the finite element model by specifying a stress-strain curve in terms of true values of stress and plastic strain. The incorporation of material nonlinearity in ABAQUS [7] requires the use of true stress, σ, versus the plastic strain, ε^{pl}, relationship, this must be determined from the engineering stress–strain relationship using:

$$\sigma = \sigma_{nom}(1 + \varepsilon_{nom}) \tag{7}$$

$$\varepsilon^{pl} = \varepsilon^t - \varepsilon^{el} = \varepsilon^t - {}^{\sigma}/_{E} \tag{8}$$

Where:

ε^{pl} = true plastic strain

ε^t = true total strain

ε^{el} = true elastic strain

σ = true stress

E = Young's modulus

σ_{nom}= engineering (nominal) stress

ε_{nom}= engineering (nominal) strain

3.2. Contact Modeling

There are several different components of the beam-to-column composite joints: the steel beam, steel column, bolts in connection zone, shear stud connectors, concrete reinforcing bars, extended end plate, column stiffeners. The contact between these components was represented using the surface-to-surface contact interaction technique as shown in Figure 5. In the directions normal and parallel to the interface plane, the HARD and PENALTY options were used, respectively [7]. A friction coefficient of 0.20 was adopted for the interface between the steel beam and concrete slab and a friction coefficient of 0.30 was used for other interactions [12].

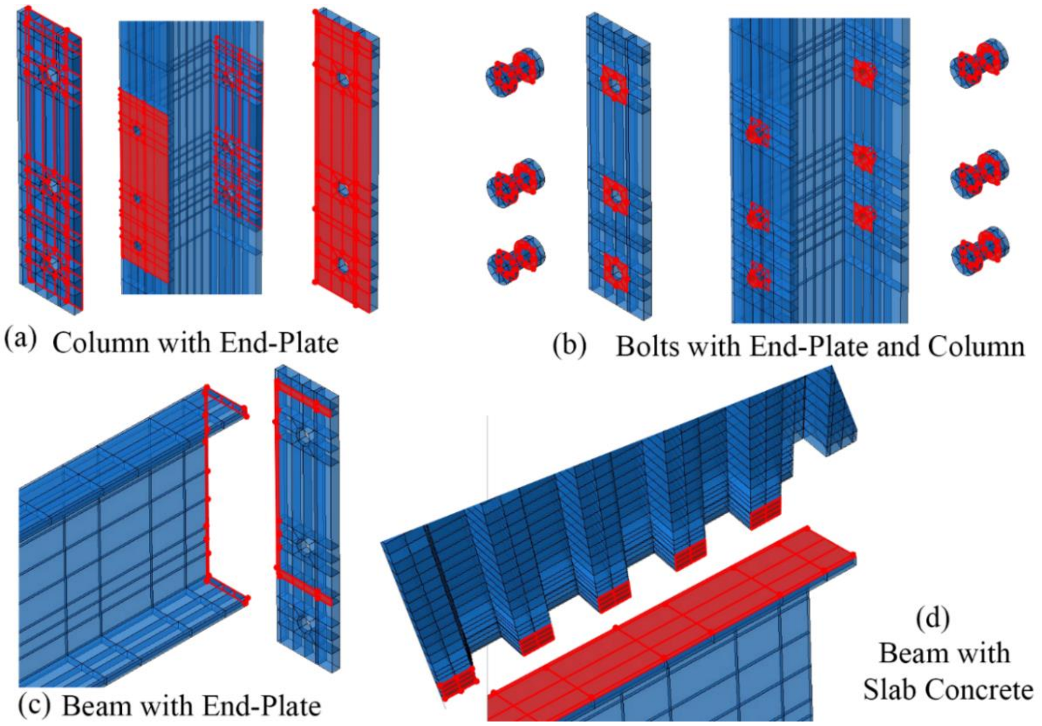

Figure 5 Contact surfaces between joint components.

The TIE option [7] was used to define the contact between the extended end plate and steel beam; the steel beam and stiffeners; and the steel column and its stiffeners to simulate perfect welding conditions between these elements.

In order to simulate the interaction between the reinforcing bars and concrete slab, the EMBEDDED option [7] was adopted, in which the reinforcement was assumed to be embedded into the concrete slab.

Finally, to simulate the shear stud connectors, non-linear springs were used, in which the results from push-out tests on M16 and M19 [5] were employed to characterize the load-slip behaviour of the shear stud connectors. The same locations of shear stud connectors were considered for the position of the springs as shown in Figure 6.

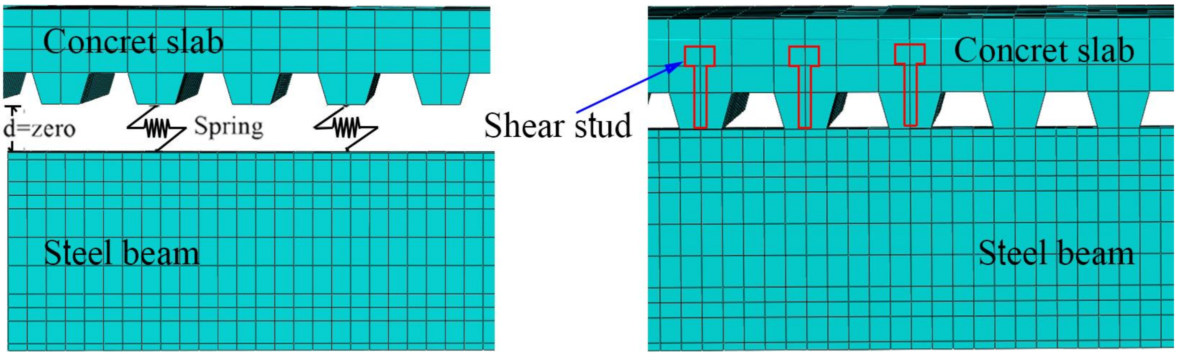

Figure 6 Simulation of shear stud connector (non-linear spring).

3.3. Meshing

An eight node linear hexahedral solid element with reduced integration and hourglass control (C3D8R) was used for modeling steel and concrete components [7]. A truss elements (T3D2) was used to model rebars [7]. The mesh configuration used for each component of the composite joint was chosen based on an extensive sensitivity analysis conducted beforehand, which is not reported here for brevity. Three-dimensional finite element meshes for the composite joint components are illustrated in Figure 7.

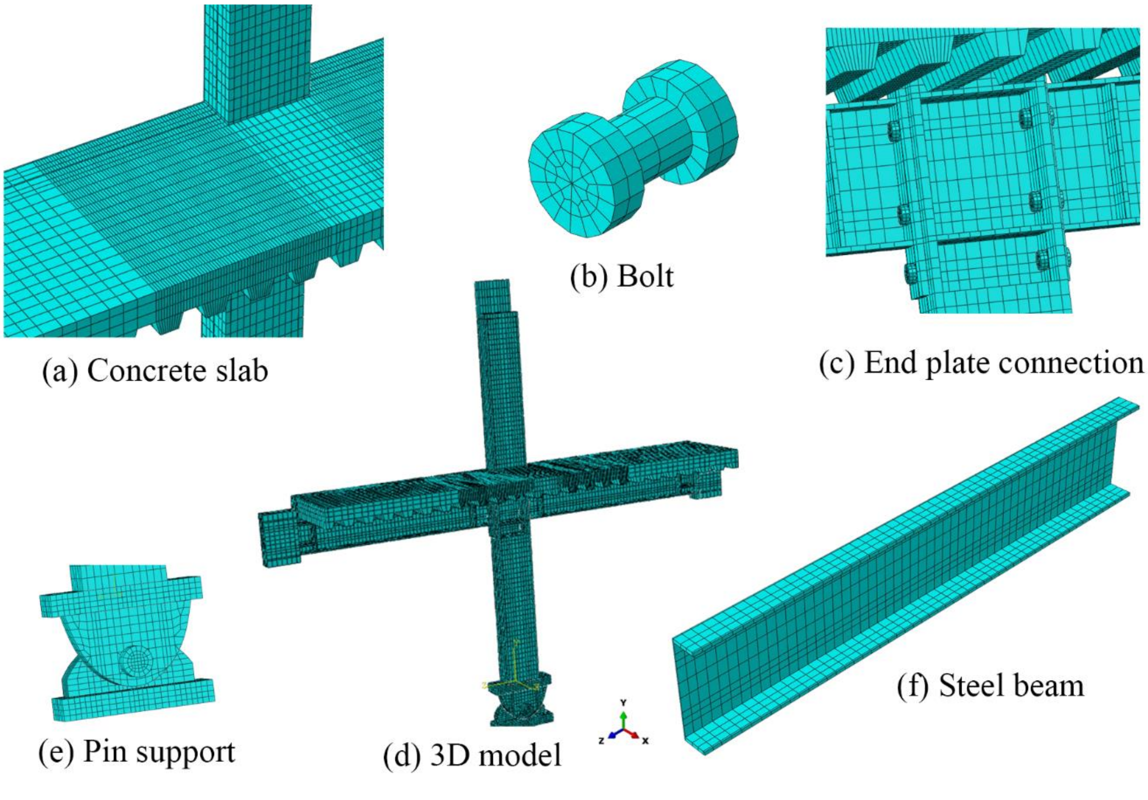

Figure 7 Mesh for interior model

3.4. Boundary Conditions and Loads

Due to symmetry in geometry and loading, only one half of the interior specimen was modeled. The associated symmetrical boundary conditions were considered on the plane of symmetry, as illustrated in Figure 8. All nodes along the middle of the concrete slab, steel column web, and longitudinal reinforcing bars were restrained from moving in the X-direction and against rotation about the Y- and Z-directions. The simulation of the pinned support at the bottom of the steel column is shown in Figure 8. A roller support was introduced at the beam ends. Supplementary, the load was applied horizontally through displacement control at the column top. The boundary conditions of the FE model are as shown in Figure 8.

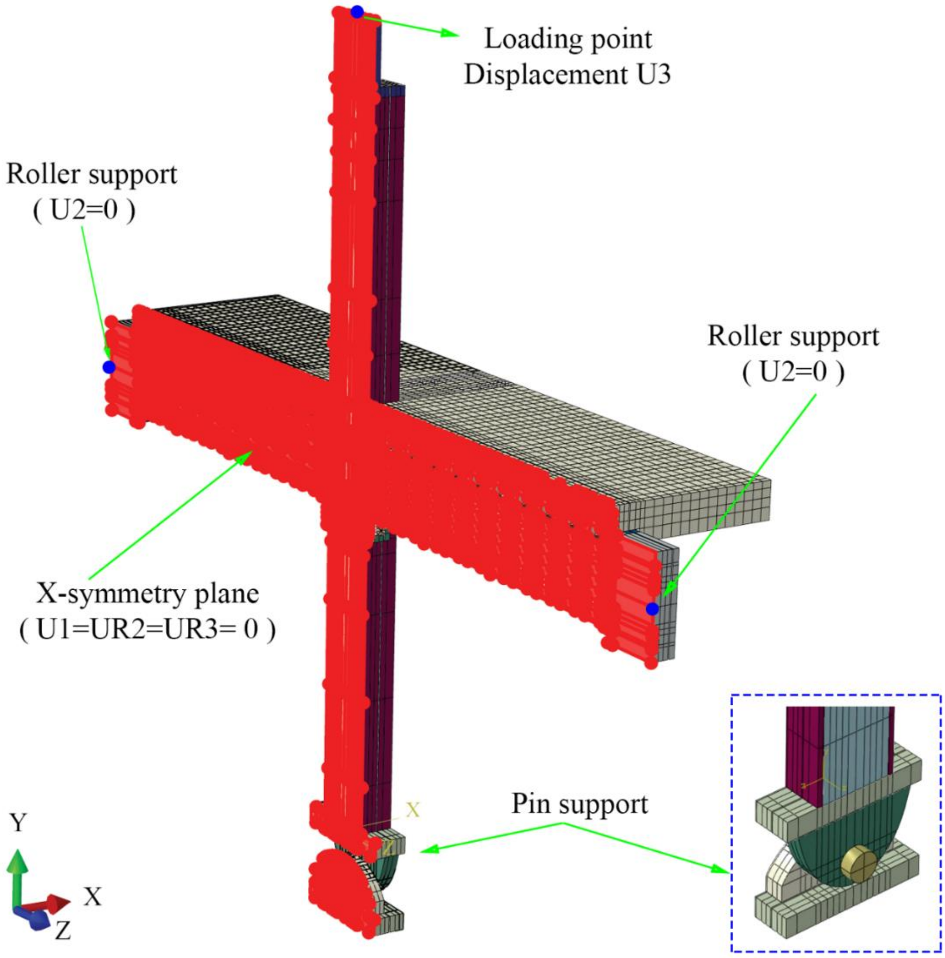

Figure 8 Boundary conditions for interior model

3.5. Load Application and Analysis Method

Loading of the specimens was conducted in two steps. In the first step, a pretension load was applied to all bolts connecting the steel beam to the column. The pretension load was 250 kN. The bolt load feature available in ABAQUS [7] was invoked in order to include the bolt pretension in this step. Following this step, the application of a monotonic displacement at the column top was applied, using the modified Riks procedure [7]. The unstable and non-linear collapse of the model can be captured using this procedure.

4. Validation of Finite Element Model

To validate the accuracy of the numerical model, the finite element analysis results were compared with full-scale test result of [12]. This investigation was directed to assess the connection behaviour and its stiffness when subjected to a monotonic loading.

4.1. Interior Joint Comparison

A comparison, in terms of applied force versus top displacement, between the experimental and numerical results for the monotonic test of interior joint is shown in Figure 9. The material model adopted for concrete limited the possibility of tracing the sudden strength reduction of the system.

A satisfactory agreement between the finite element model and experimental is obtained. Based on the behavior of these curves, it is concluded that there is a good correlation. The model can accurately simulate the initial stiffness, the point that represents the beginning of the concrete crushing (90 kN) and the ultimate load, which was 109 kN from the experimental result and 119 kN from the numerical model. The difference was 9.71%.

The deformed configuration and distribution of stresses for slab and connection is shown in Figure 10. As shown in Figure 11, the column web distortion and end plate deformation are well captured by the finite element model, compared to the experimental results.

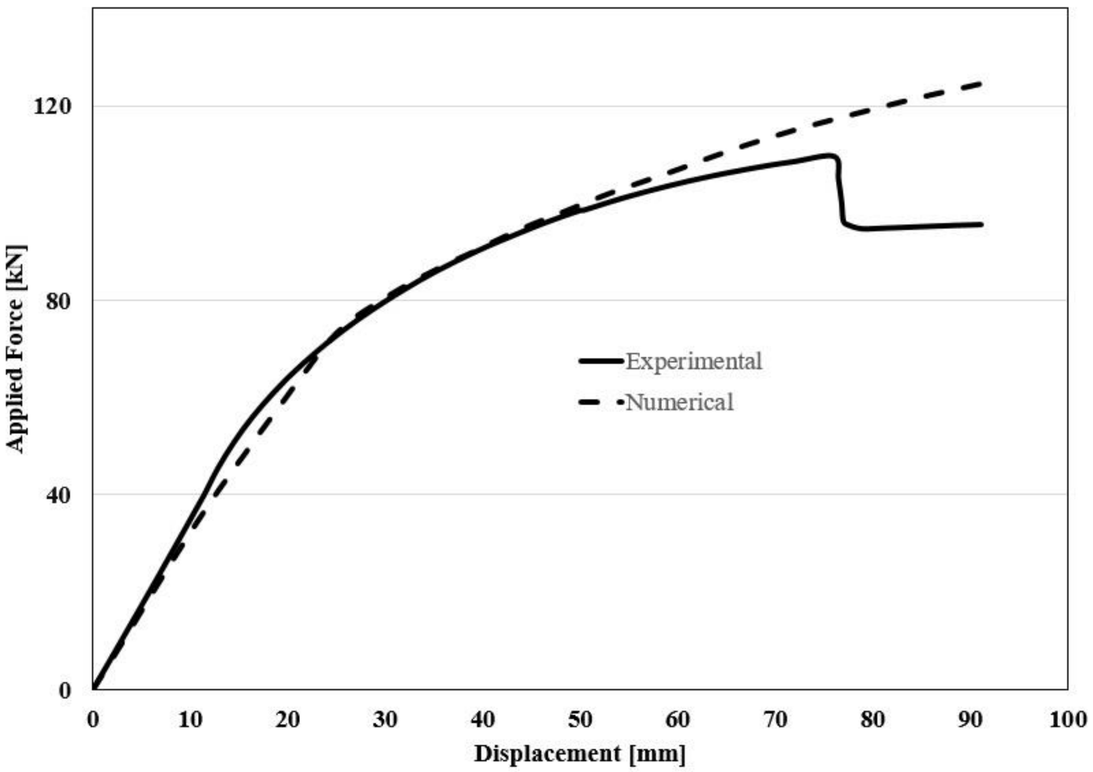

Figure 9 Comparisons between numerical and experimental results [12] of an interior joint

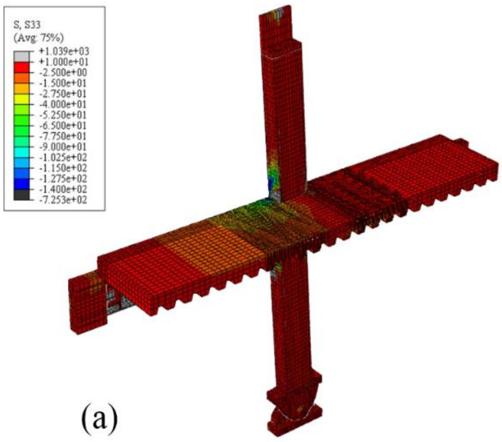

Figure 10 Deformed configuration and distribution of stresses for slab and connection

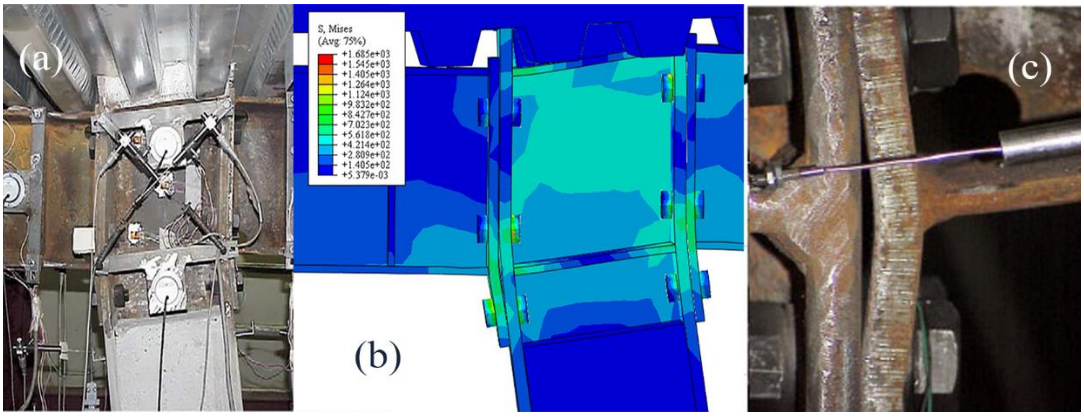

Figure 11 Comparison beteewn experimental and FE deformation results for web distorsion (a,b) and end plate deformation (b,c)

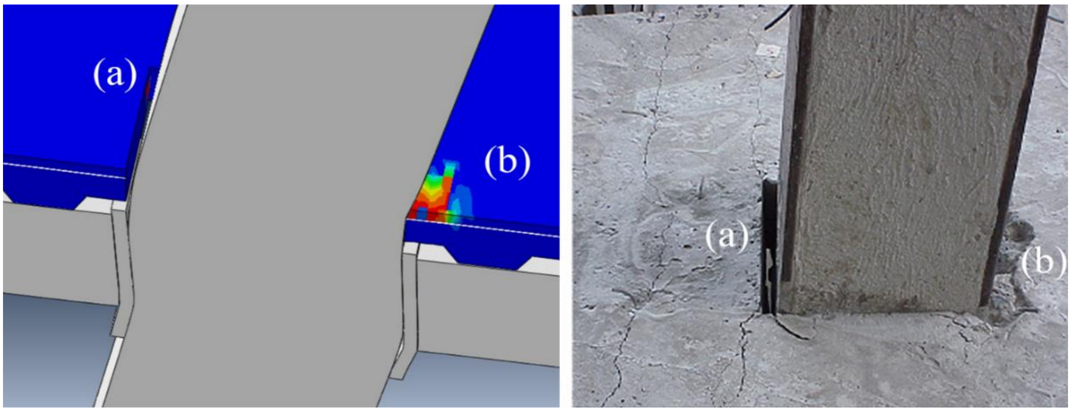

Figure 12 Monotonic response of an interior joint experimental vs finite element: (a) column sliding with respect to the concrete slab; (b) concrete slab crushing

In the experimental test [2], an inter-story drift equal to 2% marked the sudden loss of moment resistance. This is because the concrete in the beam-to-column connection region has been crushed around the column flange, as shown in Figure 12.

The strut and tie (mechanism 2), as per Eurocode 8 - Annex C [14], was the only mechanism which had been activated as shown in Figure 13. However, from the finite element model results, the inclination of the strut was 20 degrees, compared to 45 degrees as per Eurocode 8 - Annex C [14]. In addition, from the finite element model, the strut is bearing against the column flange not the column web as per Eurocode 8 - Annex C [14]. The distribution of minimum principal stresses is illustrated in Figure 13.

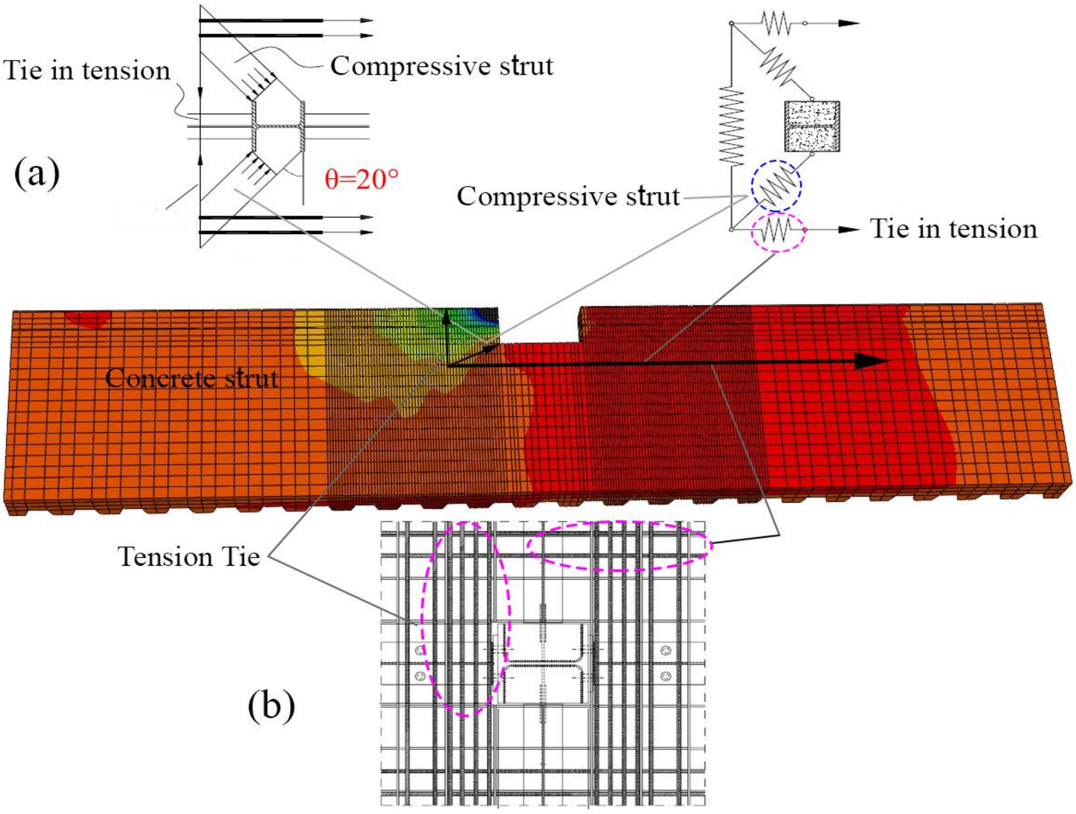

Figure 13 Mechanical models and distribution of minimum principal stresses in the concrete for an interior joint at full activation of mechanism 2

5. Summary and Conclusions

In this paper, the structural performance of composite beam to column joint has been investigated by means of an advanced finite-element numerical model (ABAQUS) [7].

The 3D finite element analysis of composite substructure under monotonic loading has allowed the composite joints to be calibrated; some inelastic phenomena characterizing their behaviour, such as the distribution of longitudinal stresses in the composite slab around the composite columns and the distribution of stresses in the column web panel and flanges, to be understood. The component models of the slab have indicated clearly that the compressive strut strength of the composite slab bearing on the column flange depends on the shear stiffness of the column web panel.

The model took into account plastic deformation developing in the beam end plate column flange as well as in the column panel zone. Longitudinal slip between the concrete slab and the beams was included and a rebar representation was used to capture both non-uniform stress distribution and progressive crushing of the concrete slab against the column.

The strut and tie (mechanism 2), as per Eurocode 8 - Annex C [14], was the only mechanism which had been activated (for precast column) as shown in Figure 13.

However, from the finite element model results, the inclination of the strut was 20 degrees, compared to 45 degrees as per Eurocode.

References:

[1] University of Pisa et al. Applicability of composite structure to sway frames. ECSC Project no. 7210-PR-250, Eur Report, European Community, 2004.

[2] L. Sim˜oes da Silva, R.D. Sim˜oes, P.J.S. Cruz, Experimental behaviour of end plate Beam-to-column composite joints under monotonical loading, Engineering Structure 23, 11, 1383-1409, 2001.

[3] M.A. Giz˙ejowski, W. Salah, W. Barcewicz, Experimental and numerical modelling of Steel flush end-plate beam-to-column joints. [In:] The scientific research problems of Building. Monograph publication (Eds. M. Broniewicz, J.A. Prusiel), Wydawnictwo Politechniki Białostockiej, 2, 225-232, Bialystok, 2007.

[4] Lee S-J, Lu L-W. Cyclic load analysis of composite connection subassemblages. In: Bjorhovde, Colson, Hajjar, Stark, editors. Connections in steel structures II. Pittsburgh: AISC; 1991. p. 209–16.

[5] ADINA user's manual, release 8.0.2. ADINA R&D Inc., Watertown, USA, 2002.

[6] Hajjar J, Leon R, Gustafson M, Shield C. Seismic response of composite moment-Resisting connections. II: Behaviour. J Struct Eng, ASCE 1998;124(8):877–85.

[7] ABAQUS Standard User's Manual. The Abaqus Software is a product of Dassault Systems Simulia Corp., Providence, RI, USA Dassault Systems, Version 6.14, USA; 2014.

[8] Doneaux C. Parametric study of the behavior of composite beams in joints to exterior Columns. In: Proceedings of the fourth international conference STESSA 2003. Behaviour of steel structures in seismic areas, Naples, Italy, 2003. p. 293–8.

[9] Millard A. CASTEM 2000, Guide d_utilisation. Rapport CEA 93/007, Saclay, France, 1993.

[10] Campbell S, Powell GH, Prakash V. DRAIN-3DX Base program description and user Guide. Report No. UCB/SEMM-94/07, 1994.

[11] Bursi OS, Ferrario F. Computational models for the low cycle fatigue behaviour of Composite members and joints. In: Progress in civil and structural engineering Computing. Stirling: Saxe-Coburg Publications; 2003. p. 119–48.

[12] Salvatore, W., Bursi, O. S., & Lucchesi, D. (2005). Design, testing, and analysis of high ductile partial-strength steel–concrete composite beam-to-column Joints. Computers & structures, 83(28-30), 2334-2352.

[13] Han, Q., Wang, Y., Xu, J., & Xing, Y. (2015). Static behavior of stud shear connectors In elastic concrete-steel composite beams. Journal of constructional steel Research, 113, 115-126.

[14] Eurocode 8. Design provisions for earthquake resistance of structures. Part 1.3: general rules. Specific rules for various materials and elements. Brussels, Belgium: CEN, European Committee for Standardization; 2004.

[15] Eurocode 4. Design of composite steel and composite structures. Part 1.1: general rules And rules for buildings. Brussels, Belgium: CEN, European Committee for Standardization; 2008.